JOURNAL OF CATALYSIS 22, 158–170 (1971)

The Catalytic Decomposition of Nitric Oxide by Metallic Oxides

E. R. S. WINTER

John & E. Sturge Limited, 1 Wheeleys Road, Birmingham, 15, England

Received June 18, 1970

The catalytic activity of 40 metallic oxides has been examined for the decomposition of NO to N_2 and O_2. Under conditions where the O_2 formed was continuously removed (as NO_2) the reaction was first order with respect to NO pressure. Proposed kinetics involve a rate-determining attack by NO upon a surface R_2-center (adjacent anion vacancies each containing a trapped electron) followed by desorption of O_2 thus re-forming the R_2-center. The parameters and rate at a given temperature of the NO decomposition are found to depend closely upon those of the O_2-desorption step, which is itself the rate-determining step in the isotopic exchange reaction between O_2 and the surface, previously studied on the same oxides. The reaction shows general similarity to the N_2O decomposition.

INTRODUCTION

The equilibrium,

$$2\,NO \rightleftharpoons N_2 + O_2, \qquad (1)$$

$$K = \frac{[N_2][O_2]}{[NO]^2} : \log K = a - c/T, \qquad (2)$$

is characterized by the values $a = -1.63$, $c = -9{,}452$ (*1*), which show that the equilibrium lies far to the right up to high temperatures. In the absence of a catalyst, however, it takes many days to establish the equilibrium even at 1000°C. The catalytic decomposition on metallic oxides may most plausibly be described by the equations

$$NO_{gas} \rightleftharpoons NO_{ads}, \qquad (3)$$

$$2\,NO_{ads} \rightarrow N_{2_{gas}} + 2\,O_{ads}, \qquad (4)$$

$$2\,O_{ads} \rightleftharpoons O_{2_{gas}} \qquad (5)$$

(followed by reaction between the O_2 and NO to form NO_2 in the cooler parts of the reaction system), which show that the reaction, except for the bimolecular reaction (4), should be very similar to the corresponding decomposition of N_2O. The latter involves (*2*) an adsorption step analogous to Eq. (3) and a decomposition stage

$$N_2O_{ads} \rightarrow N_{2_{gas}} + O_{ads}, \qquad (6)$$

followed by the oxygen desorption reaction (5). We have recently (*2*) reported, for a large number of metallic oxides, significant correlations between the reaction parameters for the oxide-catalyzed N_2O decomposition and those for the exchange, by an atomic mechanism, of ^{18}O between O_2 gas and the oxide surface. We have shown that the correlations exist because of the great importance of reaction (5) in the kinetic rate expression, although the rate-determining step is the decomposition equation (6). It is of interest to determine whether similar correlations exist for the NO decomposition.

There have been few earlier studies of this reaction on oxides: Fraser and Daniels (*3*) examined eight oxides, using a flow system at atmospheric pressure and a mixture of NO (10% by volume) in He; NO_2 in the product was measured by spectrophotometer. Yur'eva *et al.* (*4*) employed pure NO in a glass circulating system at pressures between 100 and 380 Torr and studied nine oxides, four of which were included in the list of Fraser and Daniels.

Fraser and Daniels found a zero-order reaction, while Yur'eva *et al.* found a second-order dependence on NO pressure. Sourirajan and Blumenthal (*5*) using a flow system at atmospheric pressure found an empirical first-order dependence upon NO pressure, employing concentrations of 300–2100 ppm in N_2 as carrier gas; however, no detailed examination of the kinetics was carried out. The catalysts studied were cobalt and copper oxide supported upon kieselguhr, alumina, or silica gel.

METHOD

a. Materials

The oxide samples were those employed in the earlier examination of the decomposition of N_2O (*2*). NO was obtained from a cylinder and was passed into the vacuum system over moist KOH pellets. It was then subjected to rigorous vacuum fractionation, with rejection of substantial head and tail fractions (*6*), before transference to a storage bulb: mass spectrometric examination revealed less than 0.05% of NO_2.

b. Kinetic Measurements

The oxides had previously been stabilized by use in studying the isotopic exchange with O_2 gas and the N_2O decomposition and were therefore merely outgassed for 1 hr in a high vacuum ($\sim 10^{-5}$ Torr) at the reaction temperature before each experiment. The temperature range for each catalyst was covered in a random fashion: 2–10 g of catalyst was used, depending on the specific surface of each catalyst and its reactivity. The powdered catalysts were contained in a silica reaction vessel attached to the constant-volume circulation system used for the study of the N_2O reaction. The rate of circulation of gas around the reaction system was in all cases sufficient to ensure that the observed reaction rate was independent of the circulation speed. The catalyst was protected on the "approach" side of the circulating gas by a trap at −78°C: on the other side the gas passed through a horizontal U-tube of moist KOH pellets to remove the NO_2. This tube was provided with ground glass cone joints and taps and a bypass pumping line so that it could be removed and filled with fresh KOH without exposing the catalyst to the air: the KOH was changed after every two kinetic runs as it was found that after four or five experiments its speed of reaction with NO_2 fell to too low a value. Most kinetic experiments were performed at a standard initial pressure of 200 Torr NO; pressure dependence was measured for 12 of the oxides over the range 50–400 Torr initial NO pressure. The volume of the reaction system was ca. 400 ml. Reactions were normally followed until more than 50% of the NO had reacted. The overall reaction studied was thus

$$4\,NO_g \rightarrow N_{2g} + 2\,NO_{2ads},$$

and the reaction was followed, in the reaction system of constant volume, by recording the decrease in pressure with time.

c. Adsorption Measurements

The adsorption of NO upon a selected number of oxides was measured by exposing the freshly-outgassed powders to measured amounts of the gas. The pressure was read, in a constant-volume system, by McLeod gauge after ca. 10 sec and again at ca. 1-min intervals. The system was calibrated with argon at each pressure over the temperature range. Measurements were performed between ca. 0.01 to 0.2 Torr and 4 Torr at each temperature: temperatures employed were such as to minimize or eliminate the effects of the reaction. A cold finger, normally cooled to −78°C, was included in the system and at the end of each adsorption this was rapidly warmed to room temperature. An excessive rise in pressure was observed if appreciable reaction had occurred; the measurements were restricted to conditions where the quantity of NO_2 condensed appeared to be equivalent to the reaction of less than 10% of the initial quantity of NO. The quantity of NO adsorbed was estimated by extrapo-

TABLE 1
SUMMARY OF EXPERIMENTAL RESULTS

Oxide	T (°C)[a]	E_0[b]	$\mathrm{Log}_{10}(A_0)$[c]	Pressure dependence	E_1[b]	E_N[b,d]
MgO	590–760	37	20.66	1.0	38	35
NiO	430–600	30	20.16	1.0	45	39.5
ZnO	680–770	41	21.29	1.0	36	42
CaO	580–720	28	18.74	—	30	34
SrO	620–750	15	17.38	—	15	23
CuO	370–490	9	14.81	1.0	22	24
Al_2O_3	650–750	38	20.33	—	45	43
Fe_2O_3	520–660	16	15.00	1.0	27	22
Cr_2O_3	680–780	23	16.25	1.0	38	40
Ga_2O_3	610–760	29	18.09	1.0	40.5	40.5
Rh_2O_3	400–560	14	16.45	—	10	34
CeO_2	640–800	18	16.56	—	26	26
HfO_2	730–830	18	15.71	—	30	30
ThO_2	580–840	14	15.02	1.0	22	30
SnO_2	650–790	19	16.00	—	27	32
TiO_2	670–870	19	15.99	—	35	39
IrO_2	330–450	16	17.91	1.0	24	30.5
Sc_2O_3	540–710	31	20.43	—	43	46
Y_2O_3	550–700	24	18.23	1.0	18.5	27.5
La_2O_3	630–830	16	16.40	—	11	20
Nd_2O_3	580–680	25	18.71	—	12	28
Sm_2O_3	550–760	14	15.85	1.0	19	23
Eu_2O_3	550–720	23	17.85	—	16	27.5
Gd_2O_3	470–650	19	16.59	—	12	26.5
Dy_2O_3	650–760	25	18.69	—	18	36
Ho_2O_3	590–760	32.5	20.97	1.0	37	40
Er_2O_3	570–700	28	18.49	—	36	39.5
Tm_2O_3	630–760	28	18.89	—	34	32
Yb_2O_3	600–720	29	18.62	—	30	32
Lu_2O_3	540–690	26	18.59	—	29	35

[a] Reaction temperature range.

[b] kcal $mole^{-1}$.

[c] Molecules cm^{-2} sec^{-1} at 200 Torr of NO.

[d] Activation energy for N_2O decomposition.

lation to zero time, a correction being made for any NO_2 found.

The adsorption of O_2 was measured upon freshly-outgassed catalysts in the same system with the omission of the cold finger, the adsorption being assumed complete when there was less than 5% change in the quantity adsorbed in 15 min.

Kinetics. The dependence of the reaction rate constant upon the initial pressure of NO was determined for 12 catalysts as indicated in column 5 of Table 1. In all cases a first-order reaction was indicated, and this was confirmed by reasonable first-order plots of the individual kinetic runs over 50–80% of the reaction on all the catalysts. It is possible to account for the first-order dependence upon NO pressure by assuming a rate-determining step,

$$NO_{ads} \rightarrow N + O, \qquad (7)$$

either or both of the atomic species remaining adsorbed until recombination to N_2 and O_2 occurs. This reaction, however, is most unlikely energetically.

We assume the reaction occurs by the attack of a gas phase NO molecule upon a surface R_2-center:

$$(e^-|\square_s^-)_1(e^-|\square_s^-)_2 + NO_{gas} \xrightarrow{k_e} (NO^-|\square_s^-)_1 + (e^-|\square_s^-)_2, \quad (8)$$

which is followed rapidly by adsorption of a second molecule of NO upon the F-center so formed:

$$(e^-|\square_s^-)_2 + NO_{gas} \rightarrow (NO^-|\square_s^-)_2, \quad (9)$$

where the subscripts denote particular adjacent surface sites.

The two neighboring adsorbed NO molecules then react:

$$(NO^-|\square_s^-)_1 + (NO^-|\square_s^-)_2 \rightarrow N_{2gas} + (O^-|\square_s^-)_1(O^-|\square_s^-)_2, \quad (10)$$

followed by desorption of oxygen reforming the R_2-center:

$$(O^-|\square_s^-)_1(O^-|\square_s^-)_2 \underset{k_2}{\overset{k_1}{\rightleftharpoons}} O_{2gas} + (e^-|\square_s^-)_1(e^-|\square_s^-)_2 \quad (11)$$

This scheme assumes the active surface participants are R_2-centers and F-centers; reasons for believing that these species and reaction (11) play a dominant part in both the isotopic oxygen exchange and the N_2O decomposition upon these oxides have been given elsewhere (*2*, *7*). Since we are here concerned with temperatures very similar to, but in general rather higher than, those employed in studying those two reactions, it is reasonable to invoke the same surface species in the reaction scheme.

If we assume that reaction (8) is rate-determining, then at the steady state, if N is the total number of active sites, v the number of R_2-centers, and a the number of O^- ion pairs, all per square centimeter of surface,

$$-\frac{d[NO]}{dt} = k_e A v P_{NO}, \quad (12)$$

where A is the area of catalyst employed and k_e is the rate constant of reaction (8). From (11) we have

$$\frac{a}{vP_{O_2}} = \frac{k_2}{k_1}. \quad (13)$$

Since

$$N = a + v, \quad (14)$$

we have, substituting for a

$$v = \frac{k_1 N}{k_1 + k_2 P_{O_2}}, \quad (15)$$

and from Eq. (12)

$$-\frac{d[NO]}{dt} = \frac{k_1 k_e A N P_{NO}}{k_1 + k_2 P_{O_2}}, \quad (16)$$

or if v is small, so that $N \approx a$,

$$-\frac{d[NO]}{dt} = \frac{k_1 k_e A N P_{NO}}{k_2 P_{O_2}}. \quad (17)$$

In a reaction system of constant volume

$$-\frac{d(P_{NO})}{dt} = \frac{k_1 k_e A N f(V) P_{NO}}{k_2 P_{O_2}}, \quad (18)$$

where $f(V)$ is a function of the volume and temperature of the reaction system.

The above analysis is very similar to that used to discuss the N_2O decomposition on the same catalysts (*2*). Continuing in the manner used there we write Eq. (18) as

$$-\frac{d(P_{NO})}{dt} = K_0 \frac{P_{NO}}{P_{O_2}}, \quad (19)$$

so that

$$K_0 = \frac{k_1 k_e A N f(V)}{k_2}. \quad (20)$$

Writing the rate constants in the form

$$\begin{aligned} k_e &= A_e \exp(-E_e/RT) \\ k_1 &= A_1 \exp(-E_1/RT) \\ k_2 &= A_2 \exp(-E_2/RT) \\ K_0 &= A_0 \exp(-E_0/RT) \end{aligned} \quad (21)$$

and assuming NA is independent of temperature, we have, by substituting in Eq. (20):

$$\log(A_0) = \log(A_e) + \log(A_1) - \log(A_2), \quad (22)$$

$$E_0 = E_e + E_1 - E_2, \quad (23)$$

and at any temperature

$$\log(K_0) = \log(k_1) + \log(k_e) - \log(k_2) \quad (24)$$

Now the reaction described by Eq. (11) is identical with the rate-determining equilibrium which we have shown (*7*) controls the isotopic exchange between O_2 gas and the surface of these oxides at temperatures very similar to (but usually rather lower than) those employed in the present work. We concluded that the desorption of O_2 was the rate-determining step in the exchange reaction so that k_1 is the rate and E_1 and A_1 above are the parameters of the exchange reaction. Thus, if the above kinetic scheme is correct, and the various assumptions and approximations not too drastic, Eqs. (22)–(24) should hold over the whole range of catalysts: in particular, if the parameters of reaction (8) and those of the adsorption of oxygen k_2 of Eq. (11) do not vary much from one catalyst to another, there should be a close relationship between the rate and parameters of the overall reaction (K_0, A_0, E_0) and those of the isotopic O_2 exchange reaction (k_1, A_1, E_1) over the whole range of catalysts, as was found in the case of the N_2O decomposition (*2*).

The kinetic expression accounts for the observed first-order dependence upon P_{NO}: the predicted inverse dependence upon P_{O_2} is not easily tested (because of the rapid reaction between O_2 and NO in the cooler parts of the apparatus) and we have not attempted to do this.

RESULTS

Table 1 summarizes the main kinetic results for 30 oxides: in addition PbO, WO_3, BeO, and In_2O_3 were inactive except at high temperatures where tests showed that appreciable reaction occurred in the empty reactor: V_2O_5 and MoO_3 were inactive up to ca. 30° below the mp; MnO_2 was inactive except at temperatures well above 350°C, at which temperature appreciable decomposition of the oxide (*in vacuo*) took place: observations upon Mn_2O_3, CdO, and "Tb_2O_3" were not reproducible. The results given for IrO_2 are those obtained in the first 10 runs; after this the oxide increased in reactivity over ca. 15 runs, until the rate at 350°C roughly equaled that at 450°C in the first series: E_0 then became ca. 28 kcal mole^{-1} but this value is accurate only to ± 4 kcal mole^{-1}, due to continuing variation in activity. In general, the remaining observations are believed accurate to ± 3 kcal mole^{-1} except for Sm_2O_3 and Sc_2O_3 where the error was at least ± 4 kcal mole^{-1}. To facilitate comparison with other reactions on the same oxides, the pre-exponential term is shown in Table 1 as molecules cm^{-2} sec^{-1} in a standard reaction volume of 400 ml at 200 Torr pressure of NO.

In considering the results, we first test the validity of Eqs. (22)–(24), assuming as a first approximation that the parameters of the adsorption of oxygen [Eq. (11)] and of reaction (8) remain constant over the series of oxides. In the Figures each oxide crystal type has been given a different symbol and this has been kept the same for all Figures: the symbols are essentially those used in earlier studies on these oxides.

Figure 1 shows the plot of E_1 vs E_0: the line drawn is the regression of E_1 upon E_0:

$$E_1 = 0.92\, E_0 + 5.83, \qquad (25)$$

with a correlation coefficient of 0.71. In spite of the high correlation, inspection shows that the grouping of the points is not good, and the remarkably close agreement of the slope with the value of unity predicted by Eq. (23) (assuming as a first approximation that $E_e - E_2$ is constant over the series of oxides) may be fortuitous. However Figs. 2 and 3 show that if we consider each group of oxides separately, Eq. (23) is approximately obeyed. The regression line of the set of 18 oxides of the M_2O_3 formula in Fig. 2 is

$$E_1 = 1.375\, E_0 - 7.39, \qquad (26)$$

with a correlation coefficient of 0.78, significant at better than the 0.001 level. Figure 3 similarly illustrates that the MO oxides of three different crystal types show some scatter while the MO_2 oxides appear to fall around a line of rather higher slope.

A similar test of Eq. (22) by plotting log (A_1) against log(A_0) shows very poor correlation, the corundum series showing no correlation: the plot is not given here. In view of this the plot shown in Fig. 4 of log (K_0) against log(k_1) at 550°C for all the oxides is of interest in illustrating the relative importance of the pre-exponential

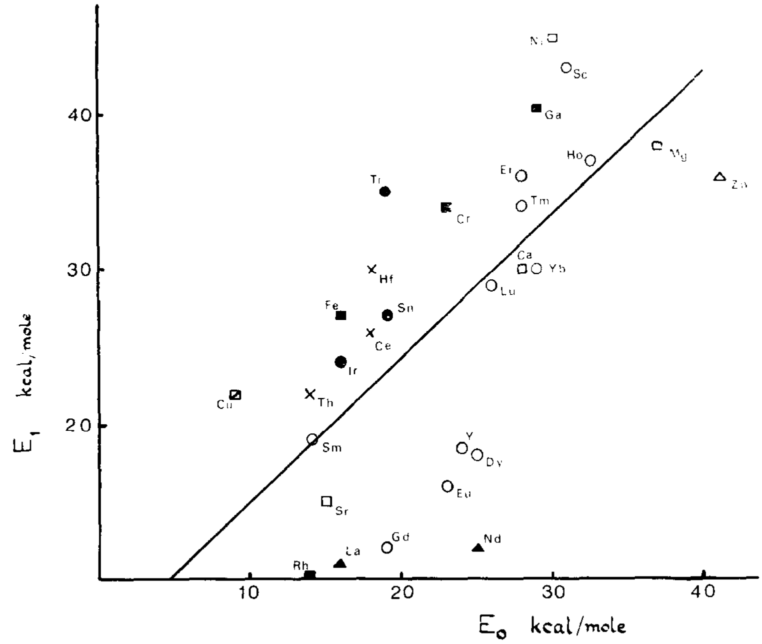

FIG. 1. E_1 vs E_0 for 30 oxides.

terms in the rate expressions of Eq. (21). A temperature of 550°C was chosen as being that which involved a minimal amount of extrapolation outside the experiment temperature ranges of the two reactions: in fact a similar plot for 650° gives very similar results. Values of the reaction rates were calculated from the data of Table 1 and of earlier papers (7). The regression line of $\log(K_0)$ upon $\log(k_1)$ is

$$\log(K_0) = 0.867 \log(k_1) + 0.314, \quad (27)$$

with a correlation coefficient of 0.61, significant at about the 0.001 level. Such a close correlation is not evident from an inspection of the plot and this is an example of the care needed in accepting statistical conclusions. It is evident that, in particular, the corundum series shows no regular trend: this shows the large effect of the pre-exponential term in the rate expression for this crystal type.

Finally we note that this reaction ex-

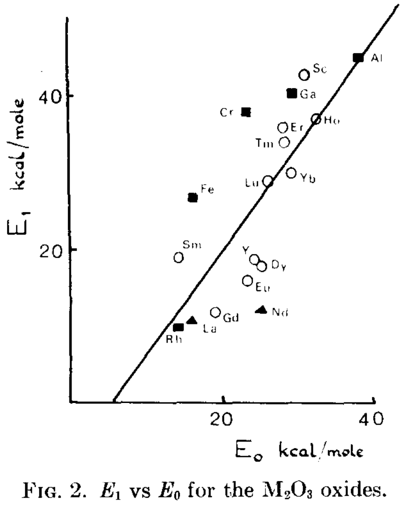

FIG. 2. E_1 vs E_0 for the M_2O_3 oxides.

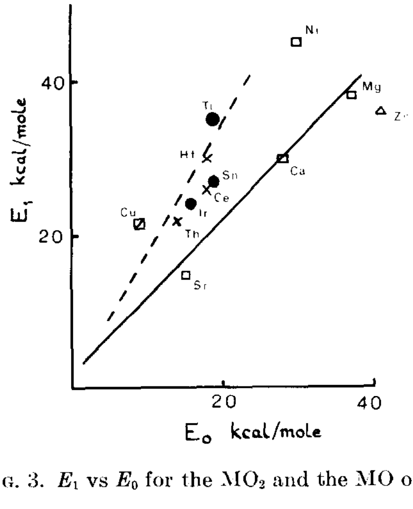

FIG. 3. E_1 vs E_0 for the MO_2 and the MO oxides.

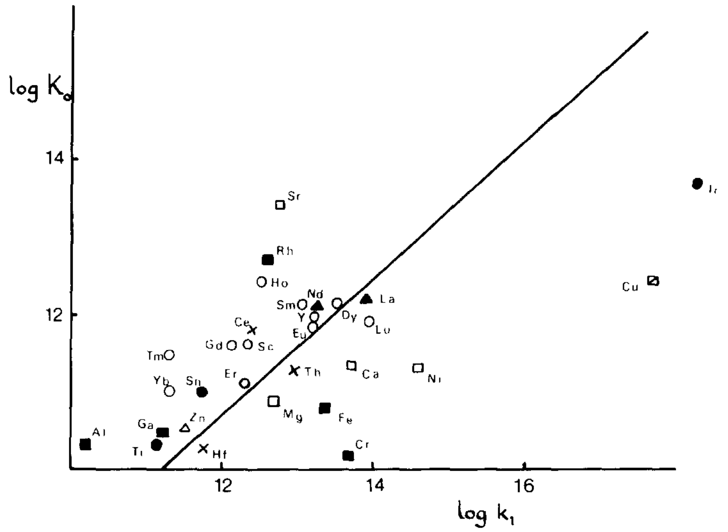

FIG. 4. Log(K_0) versus log(K_1) for 30 oxides at 550°C: rates as molecules cm^{-2} sec^{-1}.

hibits a compensation effect between E_0 and log(A_0), as shown in Fig. 5: the line drawn is the regression of E_0 upon log(A_0) and has the equation,

$$E_0 = 4.17 \log(A_0) - 50.9, \qquad (28)$$

with a correlation coefficient of 0.92.

DISCUSSION

a. *Earlier Work*

Comparison with earlier work is difficult because of the different orders of dependence of the rate upon NO pressure which have been recorded: it is not possible to be

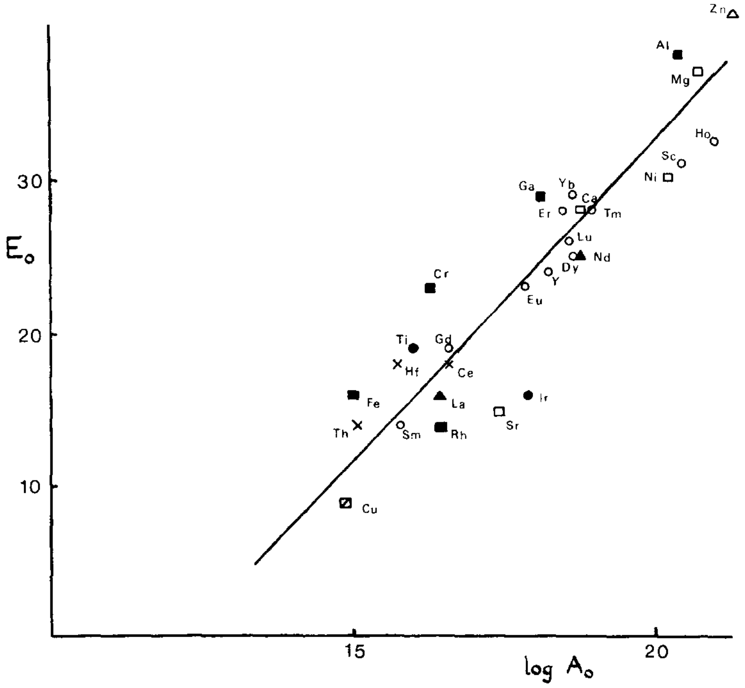

FIG. 5. Compensation-effect plot of E_0 against log(A_0) for 30 oxides.

sure of the reasons for this disagreement. The use of higher total gas pressures and He as a diluent by Fraser and Daniels (*3*) may have produced a different O_2–NO equilibrium on the surface of the catalyst from that achieved in the present work and this could account for the disagreement. Table 2 provides some evidence for a systematic difference of this nature, as excluding the inaccurate values for Cr_2O_3 and Fe_2O_3, the activation energies found by Fraser and Daniels are between 5 and 10 kcal $mole^{-1}$ lower than ours. Yur'eva *et al.* (*4*), however, found a second-order dependence upon NO pressure under experimental conditions very similar to ours. The procedure used by these workers is open to criticism: they removed the NO_2 formed by passing the circulating gas through a trap at —78°C and determined the N_2 in the product by gas chromatograph. We found that, under similar conditions of pressure, NO dissolves in the condensed NO_2 forming N_2O_3; this causes an erroneous, and in our experience erratic, increase in the rate of disappearance of NO from the gas phase. Insufficient details are given of the method of calculation of the results to assess the effect on the kinetics.

TABLE 2
COMPARISON OF ACTIVATION ENERGIES

	Apparent activation energy (kcal $mole^{-1}$)		
Oxide	Ref. (*3*)	Ref. (*4*)	Present work
Ga_2O_3	19	—	29
Al_3O_3	31.5	—	38
Cr_2O_3	(40 to 60)	20	23
Fe_2O_3	(16)	22	16
CaO	23	—	28
CuO	—	~12	9
NiO	—	20	26
ZnO	31.5	35	41

b. Importance of the Oxygen Desorption Process

The present work demonstrates that, as found for the N_2O decomposition, the oxygen desorption reaction largely controls the variation in the parameters of the NO decomposition over the range of oxides studied. Referring to Eq. (20), this means that k_1 is the dominant term, in that its variation over the series of oxides largely determines the variation in K_0. We have shown (*7*) that k_1 varies in a manner dependent upon the lattice parameter and upon the crystal type of the oxide and we therefore expect the present reaction to show very similar characteristics. We do not expect the NO decomposition to depend in a systematic fashion upon semiconductivity type, nor (as suggested by Boreskov (*8*) for reaction (11) above and a number of related reactions on Group IV oxides), upon the strength of the metal–oxygen bond. The rate constants k_2 and k_e in Eq. (20) might be expected to depend upon the Fermi level and specific chemical effects and here, presumably, is to be found the reason for the scatter in the Figures, but this aspect is not the primary concern of the present general survey.

The close parallelism between the O_2-desorption reaction and the NO decomposition is illustrated by Fig. 6 which shows a plot of E_0 against (molecular volume)$^{1/3}$ and shows close similarity to the corresponding plot for O_2 exchange (*7*): it also is very similar to the corresponding plot for the N_2O decomposition. Log(A_0) shows a moderate correlation with lattice parameter, although the correlation is better than that found with N_2O; the plot is not given here.

It may be remarked that the catalysts are, in general, much less active in promoting the decomposition of NO than that of N_2O in that higher temperatures were necessary in studying the present reaction, the decomposition of N_2O also requiring, in general, higher temperatures than the isotopic exchange between O_2 and the surface [compare the temperature ranges of column 2 in Table 1 with the corresponding values in Refs. (*2*) and (*6*)]. Thus comparison of the reaction parameters of the NO reaction with those of the oxygen-desorption reaction involves a greater extrapolation in temperature range and this, together with

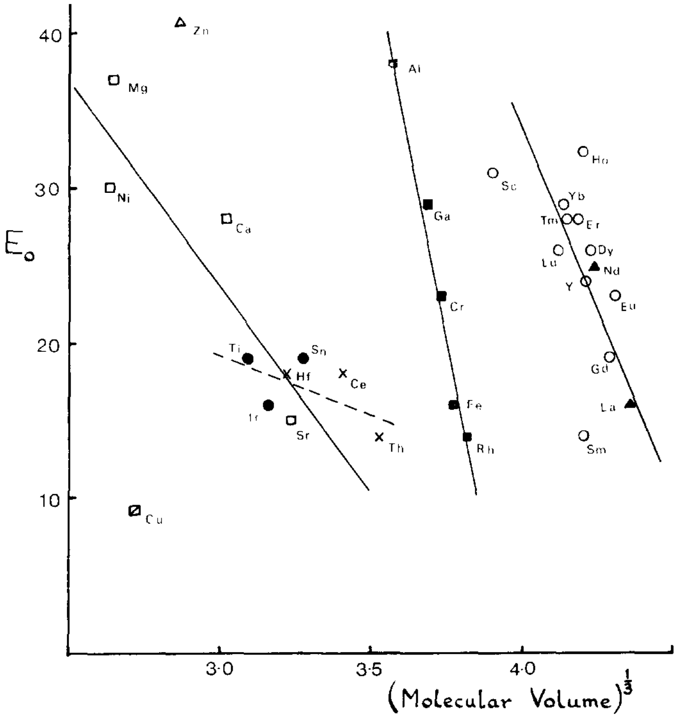

FIG. 6. Dependence of E_0 for NO decomposition upon lattice parameter and crystal type.

the different chemistry of the rate-determining step, is probably why the correlations found here are not closely similar to those found for the N_2O decomposition.

The relationships tested and to some extent found in Figs. 1, 2, 3, 4, and 6 imply therefore that k_2, k_e, etc., remain very approximately constant over the whole set of oxides: more precisely in testing Eqs. (22)–(24) we have assumed $\log(A_2) - \log(A_e)$; $(E_2 - E_e)$ and $(k_2 - k_e)$ are constant. Considering only the case of the activation energies, and comparing Eq. (25) in the form $E_0 = 1.09E_1 - 6.34$ with Eq. (23) we see that statistically $E_2 - E_e$ should be about 6–7 kcal/mole^{-1}; this is evident from Table 1 where in most cases $E_1 > E_0$. It is not possible experimentally to examine the reasonableness of this finding. When discussing the kinetics of the isotopic oxygen exchange reaction (*7*), we showed, from approximate calculations based upon the rate of bombardment of a plane surface given by simple gas kinetic theory, that it was possible for the adsorption of an oxygen molecule to require an activation energy of up to 10 kcal mole^{-1} on all the oxides, with a higher value permissible on several of those studied, including NiO where we have measured (*9*) a value of 18 kcal mole^{-1} at ca. 0.1 Torr and temperatures just below those employed in the present study. Nothing is yet known about reaction (8) above, namely the attack of gaseous NO upon an R_2-center, which we regard as the rate-determining step in the decomposition of NO. It may be that the R_2-center, because of spin-pairing of the electrons, is of roughly constant stability, at least in oxides of the same crystal habit, or this may vary monotonically with lattice spacing. Such a systematic variation might be the reason for the nonlinearity of the relationship between E_0 and E_1, for example, in the corundum and rare-earth series (cf. Fig. 2). It is probable that the larger discrepancies in Figs. 2 and 3 and the lack of correlation of the pre-exponential terms [Eq. (22)] are to be accounted for by specific chemical effects and by the difficulty of obtaining reproducible surface cleanliness in two different reactions. A comparison of the pre-exponential terms is a severe test of the theory; in the very similar case of the N_2O decomposition (*2*) the correlation of pre-exponential terms was poorer than that of the activation energies.

c. Comparison of the Decompositions of N_2O and NO

It is apparent, from a comparison of Figs. 1–4 and 6 with the corresponding Figures for the N_2O reaction (*2*), that some correlation should be found between the two decomposition reactions: this is the case. A plot of E_0 against E_N (where E_N is the activation energy of the N_2O decomposition) using the data in Table 1, gives as the regression of E on E_0

$$E_N = 0.663E_0 + 17.02 \qquad (29)$$

with a correlation coefficient of 0.90, significant at better than the 0.001 level; the plot is shown in Fig. 7. The two reactions thus follow a very similar reactivity pattern over this series of oxides, and the parallelism is sufficiently close to justify an inquiry as to how nearly the two reactions resemble each other.

The adsorption measurements summarized in Table 3 show that, in general, NO is adsorbed to a higher coverage than N_2O at roughly the same temperature and pressure. Many of the N_2O measurements are hitherto unpublished and were obtained as described in an earlier paper (*2*). Also shown in Table 3 are some values for O_2 adsorption, which shows that in many cases this gas is adsorbed to about the same extent as NO, although there are exceptions, e.g., O_2 coverage is significantly greater than that of NO on Cr_2O_3 and CuO but much less on MgO, ZnO, IrO_2 Fe_2O_3, La_2O_3, Gd_2O_3 and Er_2O_3. It is unfortunate that, due to decomposition, the adsorption measurements of NO (and of N_2O) are restricted to temperature ranges in almost all cases well below those used in the kinetic studies: the pressure range was also restricted to below ca. 5 Torr, in which region on most catalysts the coverage by NO in-

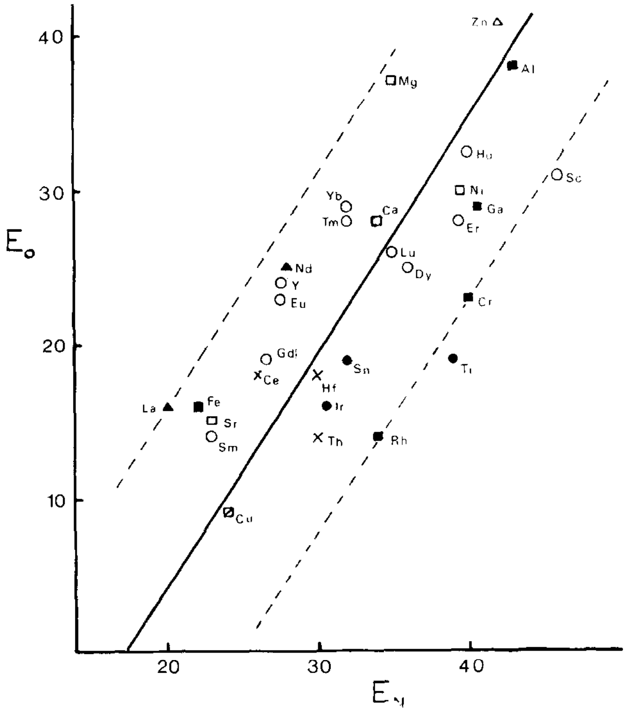

FIG. 7. E_0 vs E_N for 30 oxides; (– – –) the 95% confidence limits.

TABLE 3

Adsorption Measurements[a]

Oxide	N_2O[b]	O_2[b]	NO 0.1 to 0.2 Torr	NO 3–5 Torr	E_a
MgO	$<10^9$ (435)	1.2×10^{10} (500)	1.7×10^{11} (405)	6.1×10^{12} (500)	0
NiO	3.6×10^{12} (250)	1.2×10^{13} (320)	1.7×10^{10} (270)	6.7×10^{12} (320)	0
ZnO	3.5×10^{12} (310)	7.7×10^{11} (230)	2.1×10^{12} (150)	1.3×10^{13} (230)	0
CuO	9.0×10^{11} (22)	1.7×10^{14} (270)	5.0×10^{13} (170)	5.0×10^{13} (270)	0
Fe_2O_3	5.2×10^{10} (200)	6.0×10^{10} (470)	2.1×10^{11} (300)	9.8×10^{11} (400)	−14
Cr_2O_3	4.3×10^{10} (260)	5.6×10^{13} (410)	1.5×10^{11} (300)	8.3×10^{11} (410)	−7.5
CeO_2	2.2×10^{12} (300)	1.6×10^{13} (450)	1.6×10^{12} (350)	1.6×10^{13} (450)	0
HfO_2	1.9×10^{12} (180)	6.6×10^{12} (550)	1.1×10^{12} (445)	3.9×10^{12} (555)	0
SnO_2	5.2×10^{11} (325)	8.7×10^{12} (325)	1.5×10^{12} (180)	2.6×10^{12} (320)	0
TiO_2	6.2×10^{11} (325)	4.2×10^{12} (215)	8.5×10^{10} (215)	1.0×10^{12} (286)	0
IrO_2	5.7×10^{12} (210)	9.0×10^{13} (220)	3.0×10^{14} (175)	1.3×10^{15} (220)	0
Sc_2O_3	1.4×10^{13} (300)	7.1×10^{12} (430)	2.7×10^{11} (360)	9.8×10^{12} (430)	0
La_2O_3	—	8.8×10^{11} (545)	4.7×10^{11} (455)	3.5×10^{13} (545)	−15
Nd_2O_3	7.5×10^{11} (355)	1.8×10^{13} (410)	1.4×10^{13} (320)	3.0×10^{13} (410)	+5
Sm_2O_3	3.0×10^{12} (200)	1.1×10^{13} (460)	3.3×10^{11} (370)	1.0×10^{13} (460)	0
Gd_2O_3	1.1×10^{12} (320)	5.8×10^{11} (365)	2.9×10^{11} (300)	6.3×10^{12} (365)	+6
Ho_2O_3	—	3.3×10^{12} (530)	3.2×10^{13} (430)	1.3×10^{13} (530)	−11
Er_2O_3	—	$<10^{10}$ (500)	2.7×10^{11} (370)	1.5×10^{12} (500)	0

[a] The values in parentheses are the temperature (°C) of the measurement. The amounts adsorbed are as molecules cm^{-2}.

[b] At 2–4 Torr pressure.

creased in a roughly linear fashion with increase of pressure and showed no signs of approaching saturation. Pumping and re-adsorption measurements showed that both O_2 and NO were effectively all (>90%) strongly chemisorbed. An exception was the very active IrO_2 where, at 220°C and 4 Torr, the coverage by NO reached a monolayer in ca. 35 min; about 28% of the adsorbed gas was removed by 30-min pumping at this temperature: none of the O_2 was removed by pumping. Except for this oxide the adsorption of NO was rapid and showed no sign of an energy barrier to adsorption. The values of E_a for the adsorption process (shown as positive in Table 3 when the amount of adsorption at ca. 4 Torr increased with temperature) vary from positive to negative, in contrast with N_2O where they were all negative. The adsorption results thus indicate a more specific interaction between NO and the surface than in the case of N_2O and thus we expect, as found, a different degree of correlation between the decomposition reaction and O_2 desorption in the two cases.

Assuming that the surface complex formed on chemisorption involves the addition of an electron to the molecule being adsorbed, the difference in adsorption characteristics between NO and N_2O on a "clean" surface in the absence of oxygen may be correlated with the gas-phase reaction of these two molecules with electrons, although on adsorption the influence of neighboring ions of the oxide will not be negligible. Thus the electron affinity of gaseous NO is at least 0.65 eV (*10*) and there is no evidence of any barrier to electron attachment; while the electron affinity of N_2O is unknown (it is only possible to state (*11*) that it is probably less than that of the O atom, i.e., <1.46 eV), there is evidence of a barrier (ca. 0.21 eV) to the attachment of an electron (*12*). The lack of a barrier to chemisorption in the case of NO can also be expected since (*13*) the odd electron is more localized on the N atom than on the O atom: a relatively easy adsorption step, oxygen atom downwards, into an electron-donating surface site naturally follows.

A further difference lies in the nature of the adsorption step: we proposed (*2*) that N_2O was chemisorbed at anion vacancies or F-centers. It is possible that N_2O can also destroy an R_2-center by chemisorption:

$$N_2O_{\mathbf{gas}} + (e^-|\square_s^-)_1(e^-|\square_s^-)_2 \rightarrow (N_2O^-|\square_s^-)_1 + (e^-|\square_s^-)_2. \quad (30)$$

Since there are good grounds for believing that the free molecule-ion N_2O^- is nonlinear in the ground state (*14*), in contrast to the linear N_2O, it is likely that the decomposing charged species will effectively block the neighboring F-center until the decomposition is complete and the gaseous N_2 has moved away; the final result will most likely be an anion vacancy:

$$(O^-|\square_s^-)_1 + (e^-|\square_s^-)_2 \rightarrow (O^{2-}|\square_s^-)_1 + (\square_s^-)_2. \quad (31)$$

The kinetics of the N_2O decomposition, however, appear to indicate that the main reaction involves F-centers.

In order to promote the formation of the required reaction complex for the NO reaction, attack on an R_2-center, as in Eqs. (8) and (9) above, seems the most likely and leads in the neatest way to the correct configuration of two adjacent NO molecules in the surface, oxygen atoms downwards. We assume that adsorption of NO at an F-center or anion vacancy does not lead to reaction. Thus the formation of the reaction complex will suffer different degrees of competition with oxygen in the two cases as two different surface defects are involved. The possible reactions and equilibria between surface R_2-centers, F-centers, and gaseous oxygen at these temperatures have been discussed elsewhere in connection with the mechanism of the isotopic oxygen exchange reaction (*7*).

The decomposing reaction complexes in the two cases also make an interesting comparison: a view vertically through the surface would show the two most likely configurations, by our mechanism thus:

for the N_2O reaction showing the charged species in the bent state:

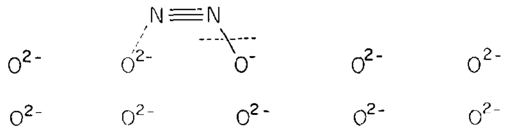

and for the NO reaction:

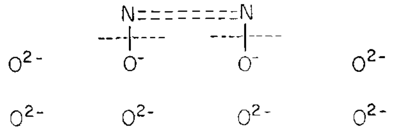

The above arguments and observations pointing to differences between the two reactions, although of some interest, unfortunately do not permit us to make even qualitative predictions about the relative apparent activation energies.

GENERAL

As with the N_2O reaction, there are likely to be no preferred active sites and no immobile areas of high or low catalytic activity, since (as is evident from the oxygen isotopic exchange work (*7*) the whole oxide surface is in a state of dynamic change which is perhaps best described as quasi-liquid. The present reaction, as in the other two cases, we regard as occurring at random all over the oxide surface. Relationships between semiconductivity properties, crystal field effects, etc., and catalytic activity upon oxides will, therefore, be much less apparent than at lower temperatures where catalytic sites might be expected to possess a more stable geometry. Such effects may, however, be apparent during the initial stages of both of these decompositions (which can usually be studied (*2*, *15*), at temperatures down to 150° below those necessary for study of the complete reaction), i.e., before the surface has become saturated with product oxygen species and the equilibrium of Eq. (11) begins to influence the kinetics. This appears to be the case in the studies by Cimino *et al.* (*15*), of the initial stages of the N_2O decomposition: here the use of alter-valent dopent ions in MgO may have two effects. First, as discussed by Cimino *et al.* (*15*), the foreign ions themselves often have a large specific catalytic activity; but, in addition, by acting as sources or traps for electrons they will affect the surface equilibrium concentration of F- and R_2-centers: the two effects may have a complex influence on the overall kinetics of both decomposition reactions. It has already been shown (*16*) that similar doping of NiO by Li increases the velocity of the oxygen isotopic exchange (i.e., oxygen desorption) reaction by factors as great as 10^3 with no appreciable alteration of the apparent activation energy, and that this is reflected in the parameters of the N_2O decomposition.

ACKNOWLEDGMENT

I thank Mrs. H. M. Westcott for performing the greater part of the experimental work.

REFERENCES

1. Moelwyn-Hughes, E. A., "Physical Chemistry," p. 989. Pergamon, London, 1961.

2. Winter, E. R. S., *J. Catal.* **15**, 144 (1969); **19**, 32 (1970).

3. Fraser, J. M., and Daniels, F., *J. Phys. Chem.* **62**, 215 (1958).

4. Yur'eva, T. M., Popovskii, V. V., and Boreskov, G. K., *Kinet. Katal.* **6**, 941 (1965).

5. Sourirajan, S., and Blumenthal, J. L., *Actes Congr. Int. Catal., 2nd,* **1960**, 2521 (1961).

6. Dodd, R. E., and Robinson, P. L., "Experimental Inorganic Chemistry," p. 233. Elsevier, Amsterdam, 1954.

7. Winter, E. R. S., *J. Chem. Soc.*, London **1968**, 2889; **1969**, 1832.

8. Boreskov, G. K., *Advan. Catal. Relat. Subj.* **15**, 332 (1964).

9. Winter, E. R. S., *J. Catal.* **6**, 35 (1966).

10. Stockdale, J. A. D., Compton, R. N., Hurst, G. S., and Reinhardt, P. W., *J. Chem. Phys.* **50**, 2176 (1969).

11. Paulson, J. L., *Advan. Chem. Ser.* **58**, 28 (1966).

12. Warman, J. M., Fessenden, R. W., *J. Chem. Phys.* **49**, 4718 (1968).

13. Walsh, A. D., *J. Chem. Soc.*, London **1953**, 2272.

14. Ferguson, E. E., Fehsenfeld, F. C., and Schmeltekopf, A. L., *J. Chem. Phys.* **47**, 3085 (1967).

15. Cimino, A., Bosco, R., Indovina, V., and Schiavello, M., *J. Catal.* **5**, 271 (1966). Cimino, A., and Indovina, V., *J. Catal.* **17**, 54 (1970).

16. Winter, E. R. S., *Discuss. Faraday Soc.* **28**, 183 (1959).